

A THEORETICAL MODEL OF PITTING CORROSION USING A GENERAL PURPOSE FINITE ELEMENT PACKAGE

Suhaila Salleh¹, Nicholas P.C. Stevens²

¹Faculty of Mechanical Engineering, Universiti Teknikal Malaysia Melaka,
Hang Tuah Jaya, 76100 Durian Tunggal, Melaka, Malaysia.

²Materials Performance Centre, University of Manchester,
Manchester M13 9PL, United Kingdom

Email: ¹suhaila@utem.edu.my, ²nicholas.stevens@manchester.ac.uk

ABSTRACT

Pitting corrosion is one of the most destructive types of metal loss. This paper presents the mathematical model of the propagation of pitting corrosion using a commercial finite element program. In view of the chemical and electrochemical reactions inside a single pit in steel, a two dimensional model that allows the prediction of pit evolution is developed. The results are discussed in comparison to Pourbaix diagram of iron and also discussed in the light of results obtained from published work reported in literature.

KEYWORDS: *Pitting corrosion, model, steel, simulation.*

1.0 INTRODUCTION

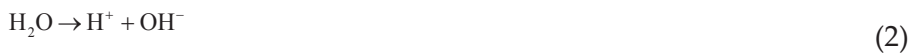
Pitting is one of many types of highly localized corrosion where small holes or cavities are formed on a metal surface but the bulk of the surface remains unattacked. A pit can be difficult to detect given that it has a tendency to undercut the metal surface and is usually covered by corrosion product. Pitting can be very destructive due to the fact that pits can cause perforation to the metal. Pits can occur in isolated locations or be so concentrated that it looks like uniform attack (Fontana 1987; Shreir 2000; Shreir 2000; Perez 2004; Ahmad 2006). Besides aqueous solution, studies have found that pitting is induced by the presence of halides, such as chlorides or bromides (Cui 2001). It is also found that pitting often occurs in situations where general corrosion is prevented by passive oxide film formed on the surface of metal (Cheng 2000). The oxide film can break down and is able to self-repair. However, sites that are not able to repair itself are liable for localized corrosion to

happen. With the presence of halides, rigorous corrosion occurs and it is established that the pH inside a pit drops to a value way below that of the bulk solution. It is also established that there are three stages of pitting (Burstein 1993; Laycock 2001; Perez 2004; Ahmad 2006): (i.) initiation of pits, (ii) formation of metastable pits and (iii) stable pitting.

Even though there is a great body of literature on pitting corrosion of iron, the propagation of pitting is not fully understood. The present paper describes a modelling approach to illustrate stage (iii), which is the evolution of a single, stable pit in steel after the initiation stage. The initial objective of this study is to look at the corrosion activities inside a pit at different potentials and pH values. To do this, a commercial program, COMSOL Multiphysics, is used as a tool and the results are discussed in relation to Pourbaix diagram of iron.

2.0 METHODOLOGY

In particular, this model is developed for the evolution of single corrosion pit in carbon steel material in aqueous sodium chloride solution. According to Sharland (Sharland 1989), six aqueous chemical species are necessary to construct a basic corrosion model of iron : Fe^{2+} , H^+ , OH^- , Cl^- , Na^+ and FeOH^+ . Pickering (Pickering 1984) and Al-Khamis and Pickering (Al-Khamis 2001) have reported experimental evidence of hydrogen gas, H_2 , formation inside propagating pits. This is also included in the model of crevice corrosion done by Vuillemin *et.al.* (Vuillemin 2007). Due to the fact that the model is to be discussed in comparison to Pourbaix diagram of iron (as shown in Figure 1), more ionic species are included, namely Fe^{3+} , FeO_2^- and HFeO_2^- . The model applies the chemical reactions as stated below (Turnbull 1982; Sharland 1988; Sharland 1988):



In the case of active walls, the metal dissolution (anodic) process is given by (Sharland 1988):



This model allows the occurrence of gaseous hydrogen formation through the simultaneous occurrence of proton reduction (cathodic) process, which is given by:



As mentioned earlier, the model studies a system in sodium chloride solution. However, sodium ions, Na^+ , are not involved in the corrosion reaction, but are involved in maintaining the electroneutrality across the mouth of pit.

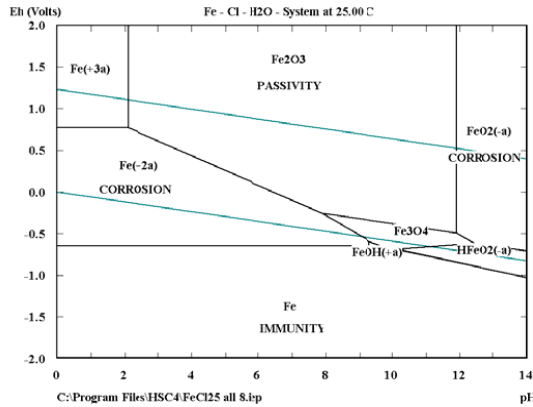


Figure 1 Pourbaix diagram of iron

The reason for adding $FeCl^+$ is to accurately model situations in which the bulk chloride concentration is large and ion pairing is likely to be significant. Furthermore, $FeCl^+$ is a stable species in standard conditions. The chemical reaction is taken as (Sharland 1988; Cottis 2004):



To obtain the respective currents for metal dissolution and reduction of H^+ , the model applies Tafel expression (Turnbull 1982; Turnbull 1982; Galvele 2005) and hence, the current density for iron oxidation, i_1 , and the current density for proton reduction, i_2 , are, respectively, given as:

$$i_1 = i_{01} \exp \left[a_1 F \frac{(V_m - V)}{RT} \right] \quad (7)$$

$$i_2 = i_{02} [H^+] \exp \left[a_2 F \frac{(V_m - V)}{RT} \right] \quad (8)$$

where V_m is the metal potential, V is the electrostatic potential in solution.

$[H^+]$ is the concentration of H^+ , a_1 and a_2 are rate constants. The metal dissolution rate and the hydrogen ions reduction rate follow Fick's First Law of Diffusion (Smith 2006) which stated that the kinetics in Equations and produce their respective fluxes (Turnbull 1987), as stated below:

$$\text{Flux of metal ions } Fe^{2+} \text{ (dissolution rate), } J_{diss} = \frac{i_1}{2F} \quad (9)$$

$$\text{Flux of hydrogen ions } H^+ \text{ (reduction rate), } J_{H^+} = -\frac{i_2}{F} \quad (10)$$

The fluxes above are now stated as:

$$J_{diss} = \frac{i_1}{2F} = \frac{0.25 \times i_{01}}{F} \exp \left[a_1 F \frac{(V_m - V)}{RT} \right] \quad (11)$$

$$J_{H^+} = -\frac{i_2}{F} = \frac{i_{02} \times [H^+]}{F} \exp \left[a_2 F \frac{(V_m - V)}{RT} \right] \quad (12)$$

where $i_{01} = 2.7 \times 10^{11} \text{ A m}^{-2}$, $i_{02} = 2 \times 10^7 \text{ A m mol}^{-1}$, $a_1 = 1$ and $a_2 = 0.5$

(Vuillemin 2007).

The chemical reactions mentioned above apply the equilibrium constants at 25°C obtained from the HSC Chemistry program. It is a chemical reaction and equilibrium software with extensive thermochemical databases.

As mentioned earlier, the initial objective of this study is to look at the corrosion activities inside a pit at different potentials and pH values. For the decrease in pH, the model examines the pH changes by incorporating the equation below and as a result, the model observes this decrease in pH:

$$\text{pH} = -\log_{10}(0.001 \times \text{abs}[\text{H}^+]) \quad (13)$$

The term inside the bracket is multiplied by 0.001 because of unit conversion from litre to cubic meter.

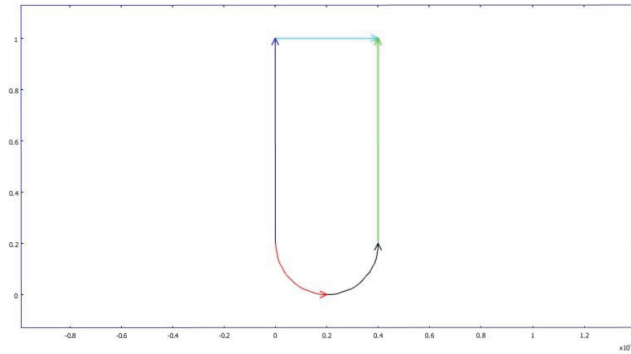


Figure 2 Geometry representing a single pit with a curved bottom

Working with COMSOL Multiphysics requires the specification of initial geometry. To represent a pit, the geometry chosen is as shown in Figure 2. Region 1 and 3 represent the passive walls, region 2 represent the mouth of the pit and regions 4 and 5 are the active bottom of the pit where metal dissolution is expected to be observed. The model applies the neutral environment of pH 7 and takes the initial chloride concentration to be 1000 mol per cubic meter. It is solved using the Nernst-Planck resolution for the range of potential between -1.5 and 1 volt.

3.0 RESULTS AND DISCUSSION

Corrosion rates of a metal can be measured by applying a current (the movement of electrical charges carried by electrons) to produce a polarization curve. The polarization curve is the degree of potential change as a function of the amount of current applied. The degree of polarization is a measure of how the rates of the anodic and the cathodic reactions are affected by various environmental conditions. Figure 3 shows that, the corrosion potential is about -0.85 volt. As potential increases, the current density, $\log i$, increases and this indicates active dissolution of metal.

Further down the pit, the pH is expected to be lower than the pH at the mouth. The higher the concentration of H^+ , the lower the pH is going to be. Figure 4 shows that as the potential increases, hydrogen

ions gradually accumulate at the bottom of the pit. This is shown in the experiment done by Lee *et.al.* (Lee 1981). The increase in hydrogen ion concentration from almost non-existent (concentration $1 \times 10^{-4} \text{ mol m}^{-3}$) to $0.0218 \text{ mol m}^{-3}$ will result in pH change. This agrees with the model which is shown in Figure 5 where the pH inside the pit drops to 4.7.

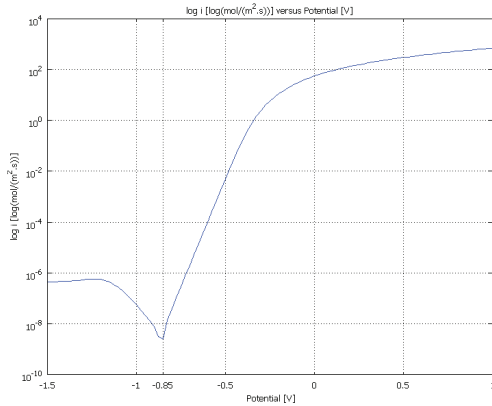
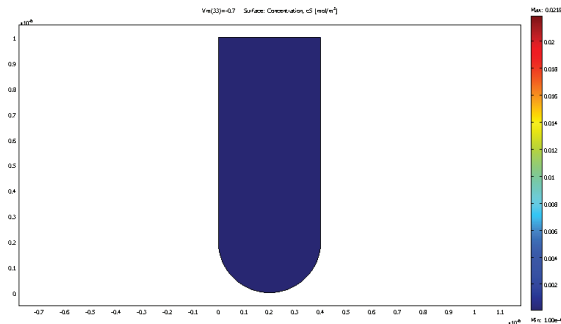
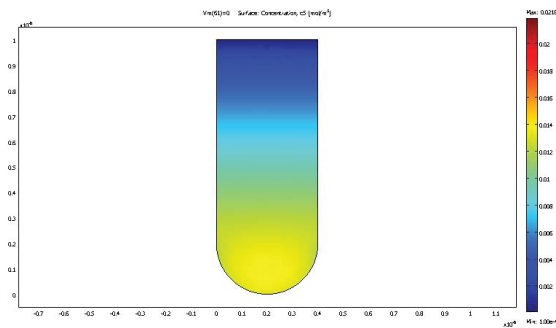


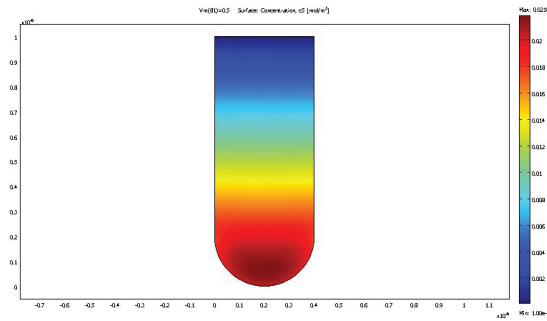
Figure 3 Graph showing the polarization curve at the bottom of pit



(i)



(ii)



(iii)

Figure 4 Graphs (i)-(iii) show the distribution of H^+ inside the pit. (i) Concentration of H^+ at -0.7 volt (cathodic). (ii) Concentration of H^+ at 0 volt (anodic) (iii) Concentration of H^+ at 0.5 volt

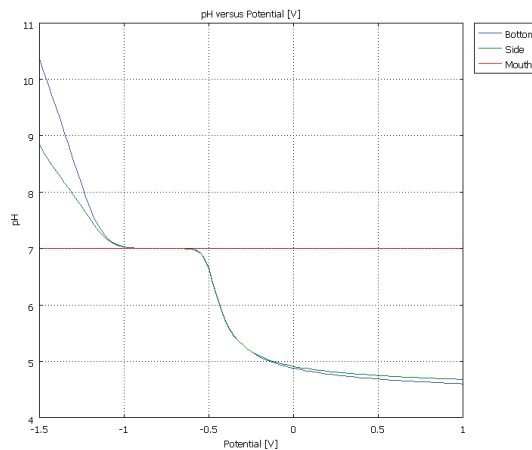


Figure 5 Graph shows difference in pH at three points along the pit

pH change still occurs at the point where the active region meets the passive region. However, the pH is shown to be slightly higher compared to the pH further down the pit. It can also be seen from the graph that at very low potential (around -1.5 volt), the condition inside the pit is very alkaline compared to the condition at the mouth. Relating Figure 3 and 5, the metal is seen to act as cathode at potential less than -0.85 volt. This is the corrosion potential, E_{corr} . At potential higher than -0.85 volt, increase in current density occurs at the region where the metal acts as cathode, as indicated by the region at the bottom of the pit. Since the increase in current density indicates corrosion activities, the pH of the purported region is expected to decrease. Sato (Sato 1995) stated that the pH in the pit is the major factor that determines the evolution (passivation or propagation) of an active pit. This is shown true by the model.

It can also be seen that as the potential increases, the slope of the current density starts to decrease starting from around -0.3 volt. This is the result of the changes in concentrations of ionic species inside the pit. It is interesting to see how one ionic concentration effects or relates to the concentration of another ionic species. Figure 6 illustrates the profiles of species concentration and shows the possible reaction occurring at different potentials. It is remarkable to see that more corrosion activities occur once water dissociates through the process of reduction. Water dissociates at potential -0.65 volt. This is explained later in this paragraph using the Pourbaix diagram in Figure 7. When this happens, the environment now has hydrogen and hydroxyl ions. The existence of hydrogen ions inside the pit attracts the chloride ions, Cl⁻, into the pit and thus, creating an acidic environment. This reaction causes the pH value to decrease (Sato 1995). When metal is placed in an acidic solution, a vigorous reaction occurs. Immediately, metal ion, Fe²⁺, is oxidized and simultaneously, reduction of hydrogen ions occurs. This is a rapid process and the hydrogen gas is expected to be seen at this stage, as shown in the experiment done by Pickering (Pickering 1984) and Al-Khamis and Pickering (Al-Khamis 2001). This is indicated in the figure below, which shows a sudden 'jump' in the 'concentration' of hydrogen gas. Meanwhile, the OH⁻ concentration is seen to decrease after -0.65 volt. This is in line with the theory of equilibrium constant of water.

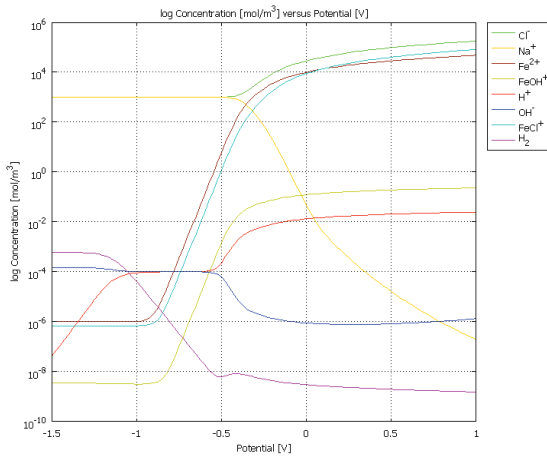


Figure 6 Profiles of concentration of all species at the bottom of the pit

The phenomenon can also be related to the Pourbaix diagram in Figure 7 shown below. At pH 7 and potential -0.65 volt, the system is crossing the Pourbaix line where the metal is crossing between two zones: zone 'immunity' into the zone 'corrosion'. This indicates that Fe²⁺ is produced

at these potential and pH condition. The presence of Fe^{2+} immediately triggers ionization of water and thus, this dissociation produces H^+ and OH^- . From the concentration profiles plot above, it can be seen that the amount of hydrogen gas starts to reduce almost immediately at potential about -0.3 volts.

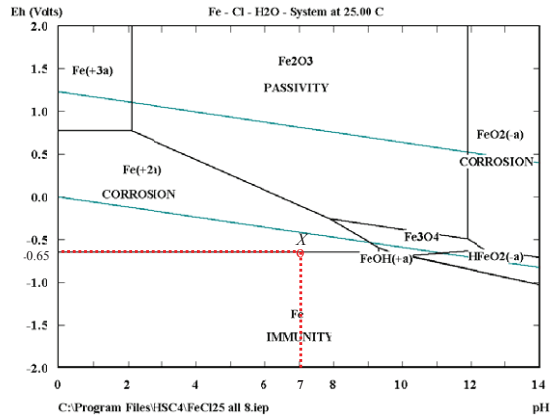


Figure7 Pourbaix diagram showing the point X where the model indicates the presence of metal ions, Fe^{2+}

From Figure 8, it can be seen that when the potential is about -0.3 volt and the pH of the system is about 5, the system is crossing line *f*, where water is thermodynamically stable rather than hydrogen gas. Below line *f*, water is reduced to hydrogen and hence, hydrogen is thermodynamically stable, just as indicated by the model.

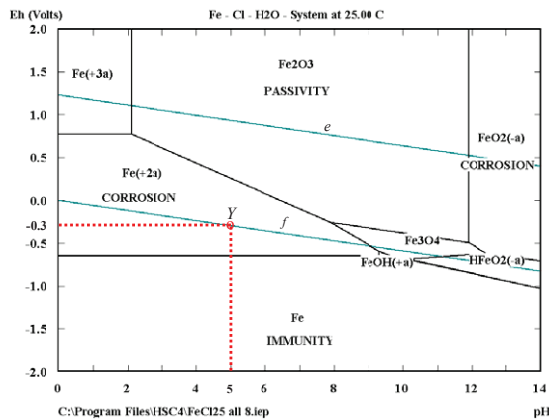
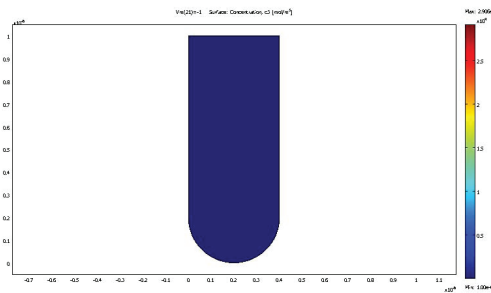
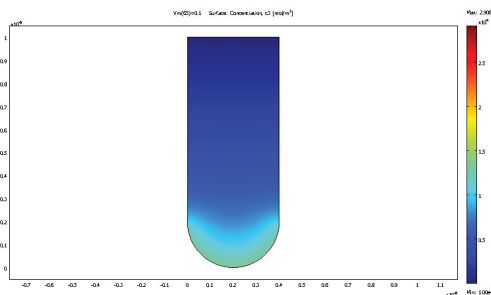


Figure 8 Pourbaix diagram showing the point Y where the model indicates the loss of hydrogen gas, H_2 , when system passes line *f*

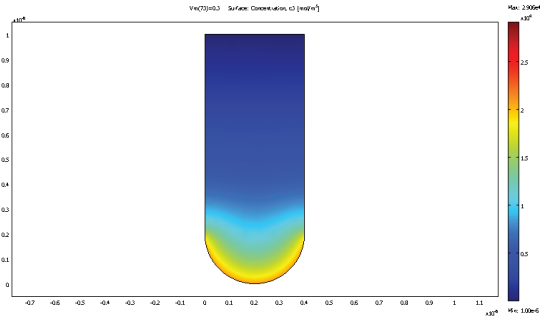
As mentioned above, the slope of the current density starts to decrease starting from around -0.3 volts. Even though this happens, the current density still maintain at a high level which indicates that corrosion of metal still occurring. From Figure 9, the concentration of Fe^{2+} at the bottom of the pit is indicated to be slightly higher than that at the side of the pit where the active region meets the passive region. Metal ions, Fe^{2+} , starts to accumulate gradually at the bottom of the pit. This is the region where the model is set to be active. Increasing concentration of Fe^{2+} at the bottom of the pit indicates that the metal dissolution is occurring continuously. From the figure also, it can be observed that Fe^{2+} starting to accumulate as we go higher up the pit. This agrees with the theory of diffusion where species move under the action of concentration gradient. This process involves species moving from high to low concentration until even concentration is achieved for all species. In this case, the concentration of Fe^{2+} has reached a limit where the metal ions diffuse to the area where the concentration of Fe^{2+} is lower which is the passive region higher up the pit. It is expected that Fe^{2+} will reach a point where it will diffuse out of the pit, as stated by Grimm and Landolt (Grimm 1994), and thus, promotes dissolution of metal, forming general corrosion to the metal surface.



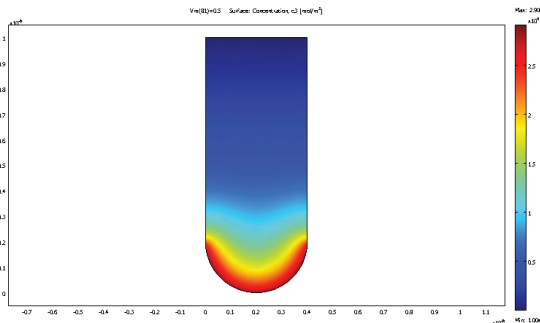
(i)



(ii)



(iii)



(iv)

Figure 9 Figure (i)-(iv) show the stages with respect to potential, where accumulation of Fe^{2+} occurs at the bottom of the pit

With the accumulation of Fe^{2+} inside the pit, this gives a positively charged environment inside the pit. This phenomenon attracts negatively charged anions into the pit through the process of migration. In this case, negatively charged chloride ions, Cl^- , migrate into the pit and this is shown by the model in Figure 10. From the figure, it is observed that the concentration of Cl^- is half the concentration of Fe^{2+} when comparing their concentration at each potential. This also agrees with the fact that Fe^{2+} has valence of 2 compared to Cl^- , which has valence 1. With increasing concentration of Cl^- inside the pit, this in turn gives a negatively charged environment inside the pit and thus, attracts the H^+ ions through the dissociation of water in the bulk solution. Accumulation of H^+ occurs inside the pit, as shown by Figure 11Error! Reference source not found.

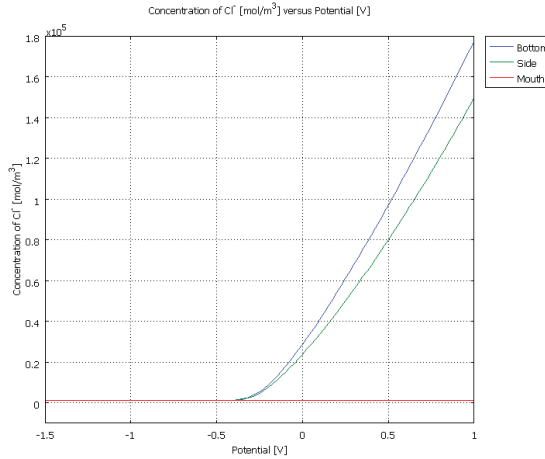


Figure 10 Graph showing concentration of Cl⁻ at three points along the pit

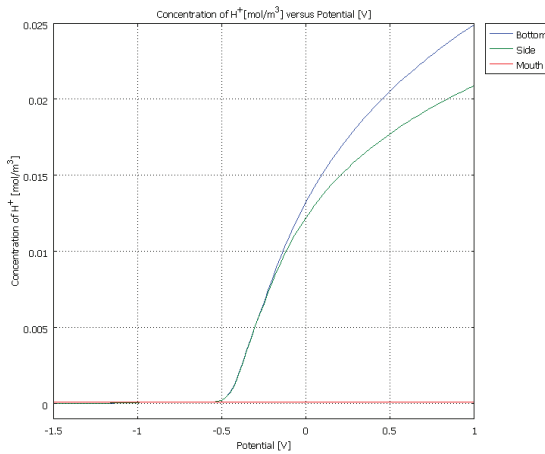


Figure 11 Graph showing concentration of H⁺ at three points along the pit

4.0 CONCLUSIONS

The model is constructed as a first step to develop a model that can represent a propagating pit. It is suggested that salt film formation and passivity are considered in the next stage of modelling.

5.0 REFERENCES

- Ahmad, Z. 2006. *Principles of Corrosion Engineering and Corrosion Control*, Butterworth-Heinemann.
- Al-Khamis, J. N., Pickering, H.W. 2001. "IR mechanism of crevice corrosion for alloy T-2205 duplex stainless steel in acidic-chloride media." *Journal of Electrochemical Society* 148(8): B314-B321.
- Burstein, G. T., Pistorius, P.C., and Mattin, S.P. 1993. "The nucleation and growth of corrosion pits on stainless steel." *Corrosion Science* 35(1-4): 57-62.
- Cheng, Y. F., Luo, J.L. 2000. "A comparison of the pitting susceptibility and semiconducting properties of the passive films on carbon steel in chromate and bicarbonate solutions." *Applied Surface Science* 167: 113-121.
- Cottis, R. A., Mousson, J.L., Vuillemin, B., and Oltra, R. 2004. "Use of a general purpose finite element package for modeling of crevice corrosion." *Corrosion* 04066.
- Cui, N., Ma, H.Y., Luo, J.L., and Chiovelli, S. 2001. "Use of general reference electrode technique for characterizing pitting and general corrosion of carbon steel in neutral media." *Electrochemistry Communications* 3: 716-721.
- Fontana, M. G. 1987. *Corrosion Engineering*. Singapore, McGraw-Hill.
- Galvele, J. R. 2005. "Tafel's law in pitting corrosion and crevice corrosion susceptibility." *Corrosion Science* 47: 3053-3067.
- Grimm, R. D., Landolt, D. 1994. "Salt films formed during mass transport controlled dissolution of iron-chromium alloys in concentrated chloride media." *Corrosion Science* 36(11): 1874-1868.
- Laycock, N. J., White, S.P. 2001. "Computer simulation of single pit propagation in stainless steel under potentiostatic control." *Journal of the Electrochemistry Society* 148(7): B264-B275.
- Lee, Y. H., Takehara, Z. and Yoshizawa, S. 1981. "The enrichment of hydrogen and chloride ions in the crevice corrosion of steels." *Corrosion Science* 21(5): 391-397.
- Perez, N. 2004. *Electrochemistry and Corrosion Science*. United States of America, Kluwer Academic Publisher.
- Pickering, H. W. 1984. Role of gas bubbles and cavity dimensions on the E-pH-ion concentrations inside cavities. *Proceeding Electrochemical Society*.
- Sato, N. 1995. "The stability of localized corrosion." *Corrosion Science* 37(12): 1947-1967.

- Sharland, S. M. 1988. "A mathematical model of crevice and pitting corrosion - II. The mathematical solution." *Corrosion Science* 28(6): 621-630.
- Sharland, S. M., Jackson, C.P., and Diver, A.J. 1989. "A Finite-element model of the propagation of corrosion crevices and pits." *Corrosion Science* 29(9): 1149-1166.
- Sharland, S. M., Tasker, P.W. 1988. "A mathematical model of crevice and pitting corrosion - I. The physical model." *Corrosion Science* 28(6): 603-620.
- Shreir, L. L., Jarman, R.A., Burstein, G.T. 2000. *Corrosion : Corrosion Control*, Butterworth-Heinemann.
- Shreir, L. L., Jarman, R.A., Burstein, G.T. 2000. *Corrosion : Metal/Environment Reactions*, Butterworth-Heinemann.
- Smith, W. F., Hashemi, J. 2006. *Foundations of Materials Science and Engineering*. Singapore, McGraw-Hill.
- Turnbull, A. 1987. "Mathematical modelling of the electrochemistry in corrosion fatigue cracks in steel corroding in marine environments." *Corrosion Science* 27(12): 1323-1350.
- Turnbull, A., Gardner, M.K. 1982. "Electrochemical polarization studies of BS 4360 50D steel in 3.5% NaCl." *Corrosion Science* 22(7): 661-673.
- Turnbull, A., Thomas, J.G.N. 1982. "A model of crack electrochemistry for steels in the active state based on mass transport by diffusion and ion migration." *Journal of Electrochemical Society* 129(7).
- Vuillemin, B., Oltra, R., Cottis, R., and Crusset, D. 2007. "Consideration of the formation of solids and gases in steady state modelling of crevice corrosion propagation." *Electrochimica Acta* 52: 7570-7576.